Original Research Article

Comparative Evaluation of the rheological and proppant handling capability of *Detarium microcarpum* as a viscosifier in Hydraulic Fracturing Fluid design

Abstract

The most frequent viscosifier used in hydraulic fracturing fluid design is guar and its derivatives. However, Guar leaves residues in solution, it is unstable at higher temperatures, and is not immune to market dynamics of demand and supply. This research aims to source for an alternate hydrocolloid for hydraulic fracturing fluid development. *Detarium microcarpum* (local), *Cyamopsis tetragonoloba*(imported) and polyanionic cellulose-regular PAC-R (Imported) were sourced, isolated, and used in carrier fluid design. The rheological properties of the three fluids were investigated at 27°C, 57°C, and 85°C. The rheological models were generated and compared with the imported samples as the control. Also, to analyse the proppant handling capacity of each of the carrier fluids, the geometry of the proppant grains and the rheology of the carrier fluids were used to compute the coefficient of drag, the drag force and the settling velocity of the carrier fluids.

Keywords: rheology, galactomannan, *Detarium microcarpum*, *cyamopsis tetragonoloba* , *polyanionic cellulose-regular*, settling velocity

List of Symbols

τ = shear stress

τ_y = yield point

k = consistency factor

γ = shear rate

n = flow behavior index

P_v = Plastic viscosity

θ_i = dial reading at ith RPM

N = spring constant

C_D = coefficient of drag

ρ = density of fluid

ρ_s = density of proppant

ν = settling velocity

R = radius of proppant grains

g = acceleration due to gravity=9.81ms^{-2}

R_e = Reynolds' number

B_i = Bingham number

Introduction

Hydraulic fracturing is a rock stimulation process that involves injecting fracturing fluids at high pressure and flow rates into the rock to improve permeability and build a network of pore spaces. The goal is to increase the rock's conductivity and the surface area that contributes to flow. The oil and gas industry has been able to explore the recovery of oil and gas from previously unexplored tight and ultra-tight reservoirs due to the success of hydraulic fracturing operations.

Fracturing fluids are essential in the hydraulic fracturing process for enhancing oil and gas production in porous medium. **API RP 13M (2018)** specifies that hydraulic fracture fluids must have adequate viscosity to originate and propagate hydraulic fractures, as well as to suspend and convey propping agents deep into the fracture. The following rheologically related features should be present in fracturing fluids: adequate viscosity, low treating pipe friction, shear stability, thermal stability, low to moderate fluid loss properties, and controlled degradability. The base fluid, which might be water, oil, or foam, viscosifiers or polymers; crosslinkers, breakers, and proppants are all important components of a typical hydraulic fracturing fluid. Some additives could be added depending on the fluid's characteristic quality or the reservoir's nature. Biocides, buffers, clay stabilizers, fluid loss additives, friction reducers, and surfactants are examples of such additives. This research focuses on the polymer or viscosifier, which is one of the most important components of a hydraulic fracturing fluid.

Galactomannan, as a key ingredient in biopolymers

Galactomannan is a heterogeneous carbohydrate found throughout nature. They are primarily found in the endosperm of leguminosae seeds. They are mostly made up of mannose and galactose, in varying proportions according to the species. They can be employed directly or as derivatives in their natural condition. The chemical structures, chain length, availability of Cis-OH groups, and replacements all influence the properties of galactomannans. Higher solubility is achieved by increasing substitution in the main chain. Galactomannan is an important enhancing agent in procedures that require a hydrophilic system to be thickened, suspended, coated, and so on. Because they have similar sugar compositions, galactomannan from Leguminosae seeds is a feasible alternative source for polysaccharides utilized in industries such as guar and locus bean gums. Variations in substitution degree and crosslinking ability may, however, result in distinct chemical characteristics.

J. Du et al. (2019) created a hydraulic fluid by crosslinking an ionic polymer gel (hydroxypropyl trimethylammonium chloride guar-cationic guar) with a bola surfactant fluid (bola-carboxylate polypropylene glycol). Due to the influence of the dual systems, it was claimed to have significantly better properties and distinctive traits. When the temperature rises, the viscosity of the fracture fluid rises abruptly, with remarkable self-assembly recovery from shearing. Due to the creation of a network of structure and supramolecular microspheres at varying pH, it also demonstrates pH-responsive viscosity variations and modest permeability impairment. The most used synthetic polymer, according to **(Bo, C et al 2018),** is polyacrylamide (PAM) and its variants. The polymers in PAM and its derivatives are

treated to acrylamino hydrolysis, which reduces the fluid's thermal stability. Due to the lack of crosslinkable groups, the viscosity, elasticity, and thermal stability of these polymers are severely constrained. He offered a new non-residual fracturing fluid that he developed by studying the structure of 2-acrylamido-2-methylpropanesulfonic acid (AMPS). The thermal endurance of the fluid will be improved by adding the high-temperature-tolerant groups 2-acrylamide and 2-methylenepropanesulfonic acid (AMPS) to the PAM. Additionally, the carboxyl provided by the acrylic acid incorporated into the polymer molecules is capable of crosslinking with the multivalent transition metal ion, increasing the viscosity of the fluid. **(Zhang, Y 2019)** proposed a new fracturing fluid that would overcome the drawbacks of guar and its derivatives (high insoluble residue, poor shear resistance, and pore throat plugging), viscoelastic surfactants VES (loss of filtrates, difficulty in breaking gel, and high fluid cost), and the Hydrophobic associating water-soluble polymer HAWSP (high insoluble residue, poor shear resistance, and pore throat plugging) (high initial viscosity, equipment damage before operation). Prior to this study, some researchers claimed that sacrificing viscosity for high elasticity outweighs any benefit that a high viscosity might provide, because high elasticity improves sand carrying capacity and reduces friction between the fluid and the equipment. Hydrophobic association interactions, electrostatic bridge effects, hydrogen bonds, and Van Der Waal forces can all help increase the elasticity of polymer solutions. HELV was made by copolymerizing acrylamide (AM), acrylic acid (AA), 4-isopropenylcarbamoylbenzene sulfonic acid (AMBS), and N-(3-methacrylamidopropyl)-N, N-dimethydodecan-1-aminium (DM-12). By incorporating a benzene ring, sulfonates, and long hydrophobic chains into the polymer structure, a copolymer solution with low viscosity and great flexibility was created. A new hydraulic fracturing fluid with exceptional viscoelasticity and thixotropy was developed**. (Zhao, L et al 2019)** proposed a novel sort of fluid that injected two types of liquid at the same time with no proppant. Fracturing fluid and supporting solids are the two forms of fluid. At high temperatures, a type of fluid known as phase change liquid (PCL) will solidify and serve as a proppant to prevent fracture closure. The second non-phase change liquid (NPCL) undergoes no phase shift during the fracturing process and functions similarly to standard fracturing fluid. **(Antosik, A 2017)** investigated the effects of hydroxyl groups and oxygen atoms on the rheological and electrokinetic features of shear thickening time as a function of chain length and branching of carrier fluid (STF). Carrier fluids included ethylene glycol, triethylene glycol, 1,3-propanediol, glycerine, poly (propylene glycol) of various molecular weights, and poly(propylene glycol) triol (dispersants). The solid phase was silica powder with an average particle size of 100nm. He measured the zeta potential, particle size distribution, steady state, and dynamic rheological properties. The findings reveal that varying the number of -OH group and oxygen atoms, as well as chain length and branching of carrier fluids, has a substantial impact on intermolecular interactions and that rheological features of a hydraulic fracturing fluid may be controlled. High viscosity friction reducers (HVFRs), which are typically high molecular weight polyacrylamides, have been recommended as a biopolymer alternative **(Geri M, Imqam A, and Flori R 2019)**. In over 26 case studies, the fluid demonstrated greater proppant transport capabilities, nearly 100 percent maintained conductivity, cost savings, a 50 percent decrease in chemical usage, less operational equipment on site, a 30 percent reduction in water consumption, and less environmental concerns. The control fluid in this study is PAC R, which belongs to the polyacrylamides group and is used in conjunction with guar. **(Cao X et al 2021)** looked at a new polyacrylamide-based synthetic polymer. For usage in

high temperature and high salt reservoirs, polyacrylamide-co-acrylic acid-co-2-acrylamido-2-methyl-1-pro-panesulfonic acid (P3A) was developed. At greater temperatures and salt reservoirs, they performed better than guar. They came to the conclusion that at higher temperatures, polyacrylamide is a good alternative for the thermally unstable guar.

***Detarium microcarpum* as a viscosifier**

Detarium microcarpum is a common tropical food ingredient used to change the rheology of soups in African cuisines. They serve as thickeners, emulsifiers, and stabilizers in soups, as well as imparting distinct flavors **(Uhegbu F et al 2009)**.

The polysaccharide component of the seed endosperms is responsible for the thickening qualities of these seed flours. The seed of D. microcarpum contains around 60% of a water-soluble polysaccharide, which is primarily a xyloglucan. These seeds' flours have a distinct behavior in hot water, exhibiting varying degrees of viscoelastic properties **(Uzomah A and Odusanya O 2011)**. According to the Uzomah and Odusanya, D. microcarpum seed flour contains the following components: ash (1.4–3.5%), protein (27–37%), fat (14.45–15%), crude fiber (2.76–2.9%), and carbohydrate (39–49.21%). **(Nwokocha L and Nwokocha K 2020)** hulled and dried the *Detarium microcarpum* seed at room temperature, and the endosperms were mixed into particle size and defatted in a soxhlet extractor with n-hexane for 12 hours. The flour was made from the defatted samples. Approximately 50 g of flour was extracted for 72 hours using ethanol. The ethanolic extract was then concentrated under vacuum at 45°C in a rotary evaporator until nearly 90% of the solvent was removed. This was put into a weighted crucible and dried in a heated water bath to a constant weight.

Constitutive equations used in the analysis of the carrier fluids

As standard hydraulic fracturing fluid exhibits Herschel-Buckley behavior, the fluids were thought to be Herschel-Buckley fluids at least until it could be demonstrated differently. The rheology, drag velocity, and settling velocity were calculated using the constitutive equations below.

$$\tau = \tau_y + K\gamma^n \quad (1)$$

$$P_v = \theta_{600} - \theta_{300} \quad (2)$$

$$\tau_y = \theta_{300} - P_v \quad (3)$$

$$\tau = 0.01066 \times \text{i} \times \text{N} \quad (4)$$

$$\gamma = 1.703 \times RPM \quad (5)$$

$$n = 3.32 \log \frac{\theta_{600}}{\theta_{300}} \quad (6)$$

$$k = \frac{\theta_{300}}{511^n} = \frac{\theta_{600}}{1022^n} \quad (7)$$

$$C_D = \frac{F_D}{\frac{1}{2}(\rho v^2)(\pi R^2)} \quad (8)$$

$$C_D = \frac{4gd}{3v^2}\left(\frac{\rho_s - \rho}{\rho}\right) \quad (9)$$

$$R_e = \frac{\rho v^{2-n} d^n}{m} \quad 10$$

$$B_i = \frac{\tau_o}{m(\frac{v}{d})} \quad 11$$

Equations 9, 10, and 11 can be solved using different values of the slip velocity, v by trial and error. The result can be validated using **(Atapattu et al 1995)** semi-empirical correlation for drag on spheres in Herschel-Bulkley model liquids.

$$C_D = \frac{24}{R_e}(1 + Bi) \quad 12$$

$$F_D = \frac{\pi d^3 (\rho_s - \rho) g}{6} \quad 13$$

For,

$10^{-5} \leq \text{Re} \leq 0.36$

$0.25 \leq \text{Bi} \leq 280$

$0.13n \leq 0.95$

The values of B_i, R_e, the diameter of proppant grains, the density of the proppant grains and the density of the carrier fluids are inputted into equations 12 and 13 to compute the coefficient of drag and the drag force.

Objective and Significance of the Study

The conventional hydraulic fracturing fluid viscosifier-Cyamopsis tetragonoloba (CT) and the conventional drilling mud viscosifier-PAC-R were used as benchmarks to examine the suitability of *Detarium microcarpum (DM)* as a polymer in hydraulic fracturing fluid design. The study will show how *Detarium microcarpum (DM)* compares to guar gum and PAC-R in terms of performance. In addition, using a locally available biopolymer for hydraulic fracturing fluid design would drastically reduce the cost of both the fluid design and the hydraulic fracturing process.

Methodology

Sample collection

The DM seed was bought at Rumuokoro Market,Port Harcourt, while the CT and PR were bought processed from Joechem Chemicals, Choba, Uniport.

List of Equipment

Oven, Soxhlet extractor, blender, mechanical stirrer, hammer mill, centrifuge bottle, knife, glass rod, beaker, measuring cylinder, thermometer, pH meter, Hamilton Beach mixer, Fann Viscometer, electric weigh balance, stopwatch, measuring cylinder, water Bath.

Procedure

The *Detarium microcarpum(DM)* seed is dehulled and the endosperm is pulverized using a hammer mill. A blender is used to blend the pulverized seed into a fine powder. To extract the oil from the powder, it is wrapped with crystalline filter paper and placed in a Soxhlet extractor. Propanol is used for this. In a continuous reflux procedure, the content is left in the Soxhlet extractor for three days. The resulting powder was baked for 6 hours at 80^0C in an oven.The obtained DM powder is mixed separately with the already processed CT and PR at a concentration of 10g per litre of water. The three samples are placed in a Fann viscometer, with dial readings collected at 3, 6, 100, 200, 300, and 600 RPM and 27^0C. At temperatures of 57°C and 85°C, the procedure is repeated.

The travel time of proppant sand particles of 78% 0.002m grain diameter (ASTM 10) down the burettes is taken and used as the raw data to compute the drag force and the settling velocity with DM, CT, and PR at a concentration of 10g/l in three burettes.

Data Presentation and Discussion of Results

Appendix 2 shows the rheology of Detarium microcarpum(DM), Cyamopsis tetragonoloba (CT), and Polyanionic-cellulose filtration control additive PAC R (PR) after 10 sec and 10 min in a viscometer at 27°C, 57°C, and 85°C. Equations 4 and 5 were used to convert the readings to oilfield units, which are highlighted on 4,5,6. For the diameter of the proppant sand, the sizes from sieve analysis are converted using the sieve conversion chart in appendix 1.

Table 1: Rheology of *Detarium microcarpum* at 27ºC, 57ºC and 85ºC in oilfield units

Shear strain (S^{-1})	**Stress (lbf/100ft^2) 27^0C**	**Stress (lbf/100ft^2) 57^0C**	**Stress (lbf/100ft^2) 85^0C**
1021.8	0.1599	0.1386	0.1066
510.9	0.1173	0.0959	0.0746
340.6	0.0853	0.0853	0.0640
170.3	0.0533	0.0533	0.0426
10.22	0.0320	0.0213	0.0213
5.11	0.0213	0.0213	0.0213
N	0.4472	0.5302	0.1549
K	0.0072	0.0035	0.0364

Table 1 shows the dial readings of DM at temperatures of 27°C, 57°C, and 85°C, generated using equations 1–7 from raw data on appendix 2, table 2. In Table 1, the shear strain and shear stress at 27°C, 57°C, and 85°C are computed and presented. With an increase in

temperature, DM shows a decrease in shear stress. With a reduction in shear strain, there is also a reduction in shear stress. With increasing temperature, the flow behavior index, n, and the consistency factor, k, obtained from equations 6 and 7, decrease.

Table 2: Rheology of *Cyamopsis tetragonoloba* at 27ºC, 57ºC and 85ºC in oilfield units

Shear strain (S^{-1})	**Stress ($lbf/100ft^2$) 27^0C**	**Stress ($lbf/100ft^2$) 57^0C**	**Stress ($lbf/100ft^2$) 85^0C**
1021.80	0.7569	0.6822	0.5543
510.90	0.5437	0.3731	0.2878
340.60	0.4477	0.2985	0.1706
170.30	0.3198	0.1706	0.1173
10.22	0.0640	0.0426	0.0320
5.11	0.0533	0.0320	0.0213
n	0.4772	0.8705	0.9453
k	0.0277	0.0016	0.0008

Table 2 shows CT dial readings at temperatures of 27°C, 57°C, and 85°C, generated using equations 1–7 and raw data from appendix 2, table 3. In Table 2, the shear strain and shear stress at 27°C, 57°C, and 85°C are computed and presented. With a rise in temperature, Cyamopsis tetragonoloba shows an overall decrease in shear stress. With a reduction in shear strain, there is also a reduction in shear stress. The flow behavior index of Cyamopsis tetragonoloba, on the other hand, increases as the temperature rises. However, when the temperature rises, the consistency factor drops.

Table 3: Rheology of PAC R at 27^0C, 57^0C and 85ºC in oilfield units

Shear strain (S^{-1})	**Stress ($lbf/100ft^2$) 27^0C**	**Stress ($lbf/100ft^2$) 57^0C**	**Stress ($lbf/100ft^2$) 85^0C**
1021.80	0.4690	0.4477	0.4051
510.90	0.2878	0.2452	0.2239

340.60	0.2132	0.2025	0.1812
170.30	0.1279	0.1066	0.0959
10.22	0.0320	0.0320	0.0213
5.11	0.0320	0.0320	0.0213
n	0.7043	0.8685	0.8554
k	0.0036	0.0011	0.0011

Table 3 shows the dial reading of the PAC R at temperatures of 27°C, 57°C, and 85°C, generated using equations 1–7 from the raw data on appendix 2, table 4. In Table 3, the shear strain and shear stress at 27°C, 57°C, and 85°C are computed and presented. With an increase in temperature, PAC R shows an overall decrease in shear stress. With a reduction in shear strain, there is also a reduction in shear stress. The flow behavior index has a small slant to it; it rises at 57°C and falls slightly at 80°C. The consistency factor, on the other hand, follows a predictable pattern of diminishing as the temperature rises.

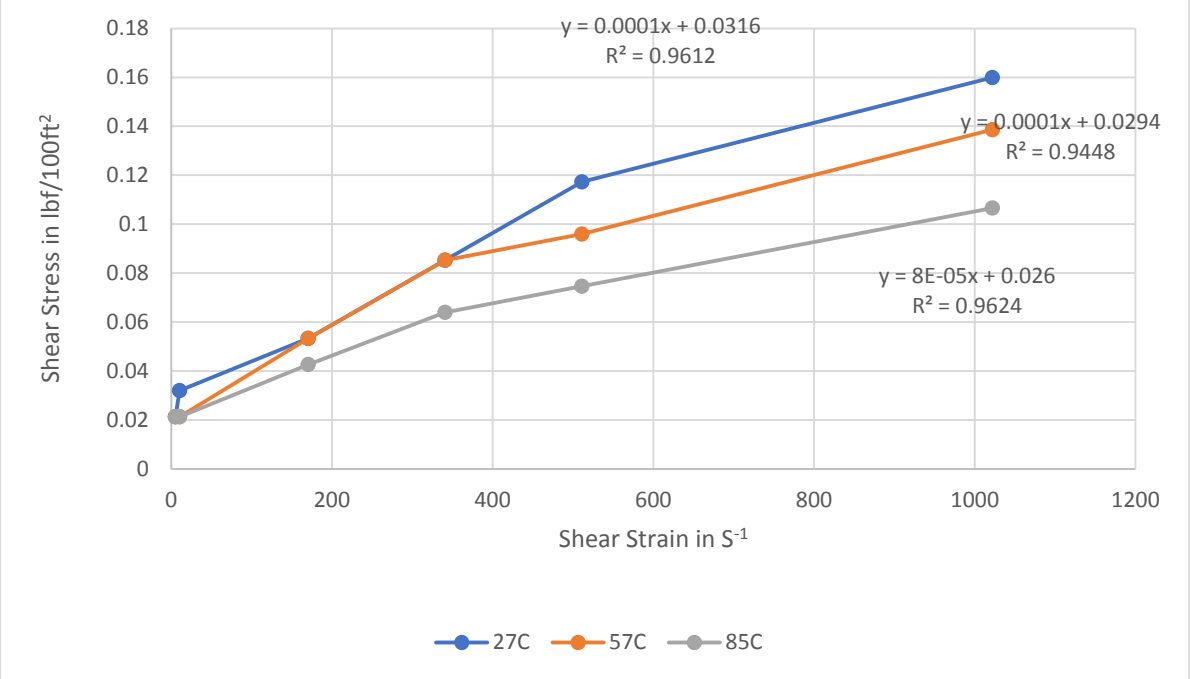

Fig. 1: Rheology of DM at different temperatures and 10g/l concentration

The DM has the best rheology at the laboratory temperature of 27^0C, as seen in Fig 1. Rheology is reduced at higher temperatures, such as 57°C and 85°C. The curves are densely

linked, which is an intriguing aspect of this discovery. It means there isn't much of a variation in rheology between 57°C and 85°C. Also, with a yield point of 0.0316 lbf/100ft^2 at 27^{0}C, the yield point is the greatest. At 57°C and 85°C, the yield points are 0.0294 lbf/100ft^2 and 0.026 lbf/100ft^2, respectively

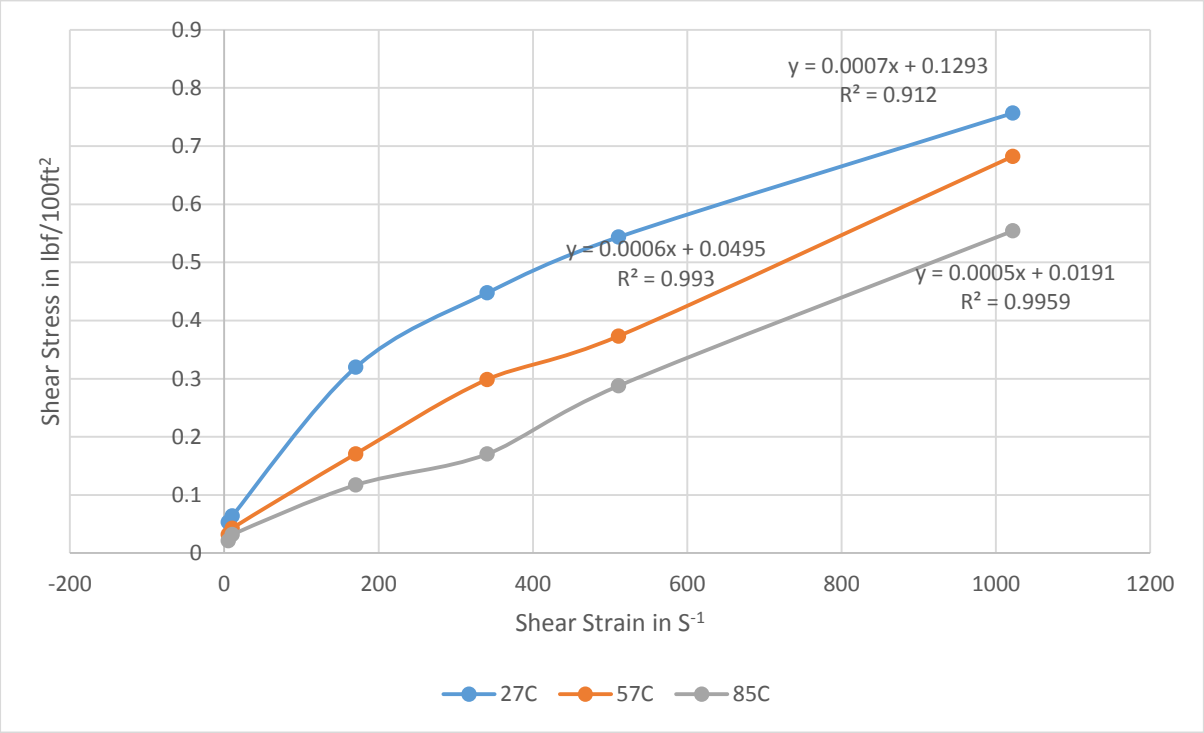

Figure 2 shows the rheology of CT at various temperatures and concentrations of 10g/l.

At 27^{0}C, the shear stress-shear strain plot (shown in fig 2) show the rheological behavior. The three temperatures are found to be equidistance. This indicates that when the temperature rises, the polymer continues to de-naturate. It means there isn't much of a variation in rheology between 57°C and 85°C. Also, with a yield point of 0.1293 lbf/100ft^2 at 27^{0}C, the yield point is the highest. At 57°C and 85°C, the yield points are 0.0495 lbf/100ft^2 and 0.0191 lbf/100ft^2, respectively.

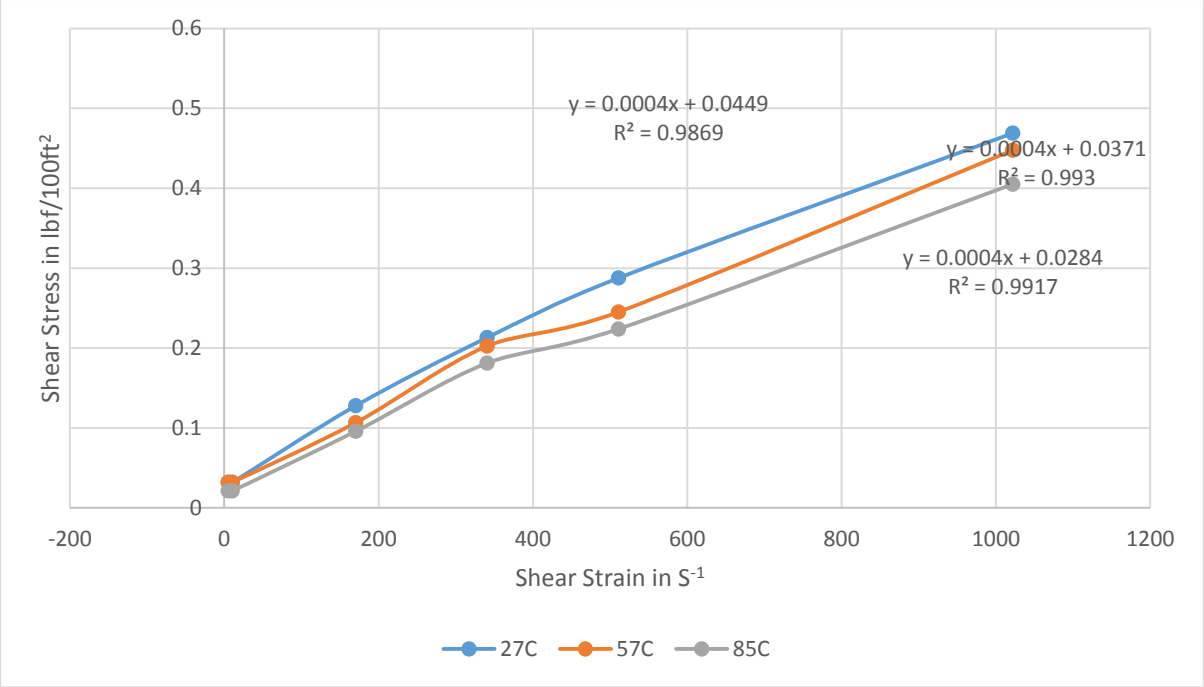

Fig. 3: Rheology of PR at different temperatures and concentration of 10g/l

The plot of shear-stress against shear-strain for the PR at various temperatures (fig 5) shows close knitted behavior at lower shear strains and equidistance close-knitted behavior at higher shear strains. It means there isn't much of a variation in rheology between 57°C and 85°C. Also, with a yield point of 0.0449lbf/100ft^2 at 27^{0}C, the yield point is the highest. At 57°C and 85°C, the yield points are 0.0371lbf/100ft^2 and 0.0284lbf/100ft^2, respectively.

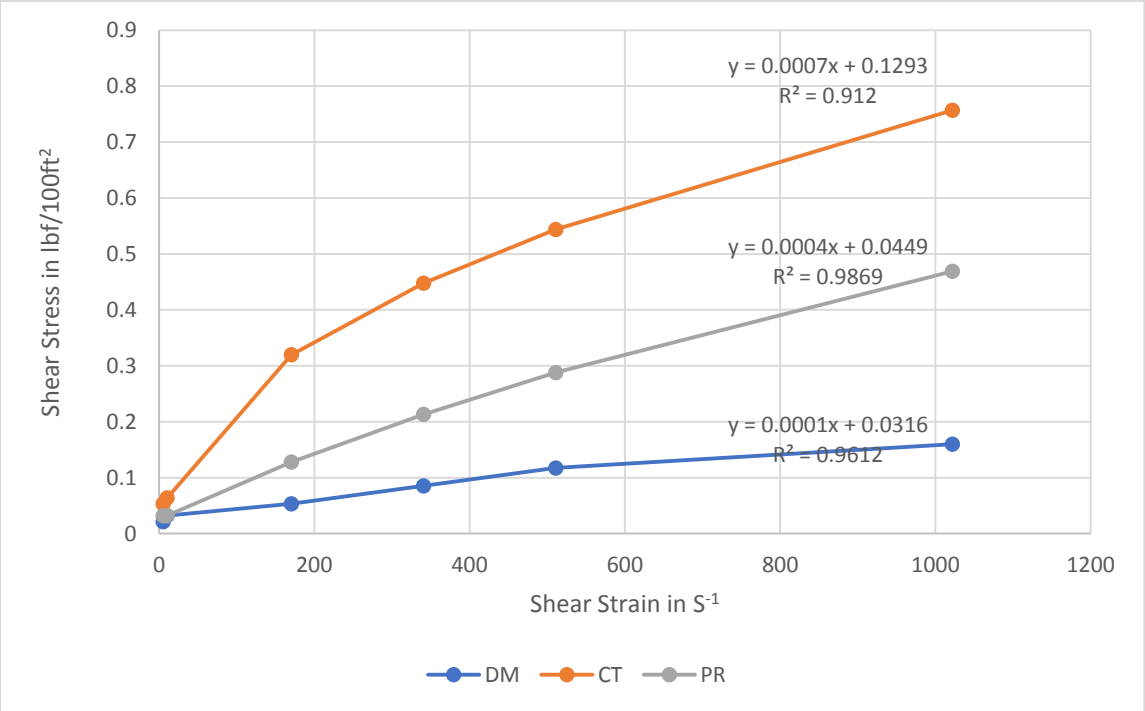

Fig. 4: Rheology of DM, CT, and PR at 27^0C and 10g/l concentration

At 27°C, the three biopolymers are shown in Figure 4. The best rheology is seen in CT, followed by PR, and finally DM. The rheology of the three biopolymers also shows an equidistance difference. This implies that there is a significant difference in their laboratory performances, CT > PR > DM. At lower temperatures, remember that CT is the industry standard. Also, with 0.1293lbf/100ft2, CT has the highest yield.

Fig. 5: Rheology of DM, CT, and PR at 57^0C and 10g/l concentration

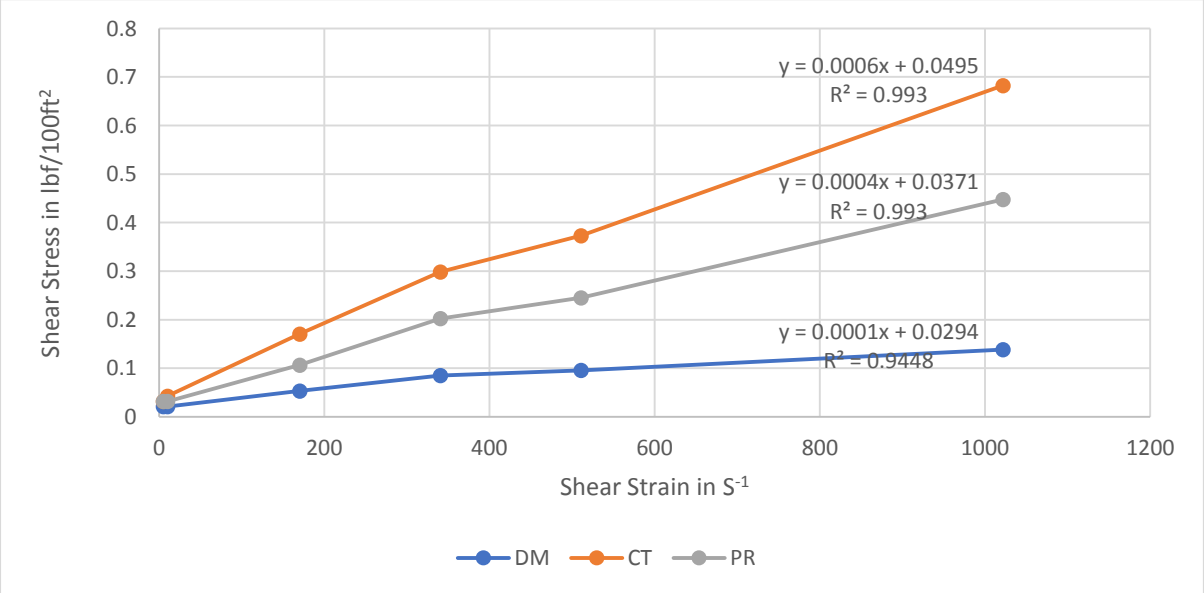

The three biopolymers are shown in Fig. 5 at 57°C. The best rheology is seen in CT, followed by PR, and finally DM. The rheology of the three biopolymers also shows an equidistance difference. The gap between the DM and PR stays as large as it was at 27^0C, however the gap between the CT and PR gradually reduces at 57^0C, indicating that PR improves at higher temperatures.

Fig. 6: Rheology of DM, CT, and PR at 85^0C and 10g/l concentration

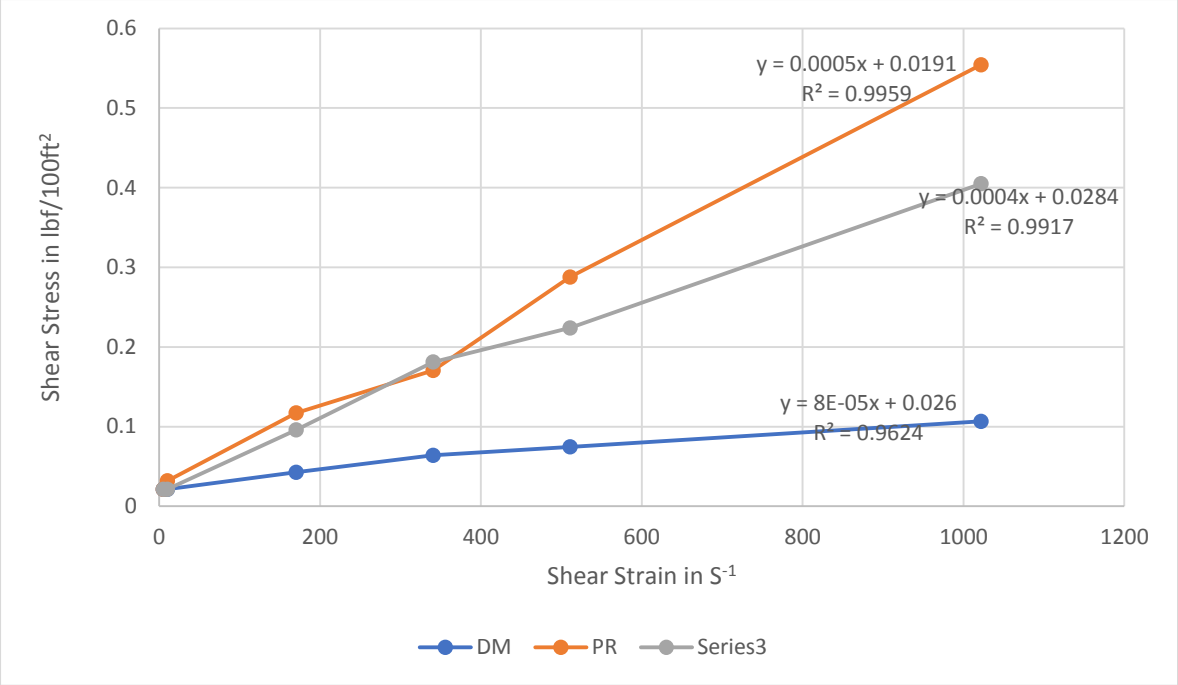

In Fig. 4, the rheological behavior of the three polymers at 27^0C in the laboratory reve aled CT to be the best by a considerable margin. The PR is a close second. The difference between CT and PR has shrunk at a higher temperature of 57^0C for fig 5, with DM still wallowing at the bottom. At 85^0C, the characteristics of CT and PR are close-knit at lower shear rates and close enough at higher shear rates, as seen in fig 6. The DM remained at the bottom of the heap. This suggests that the PR could be an effective substitute for CT in a job involving high-temperature hydraulic fracturing.

Fig 7. The Plot of the consistency index, k of the three polymers against temperature

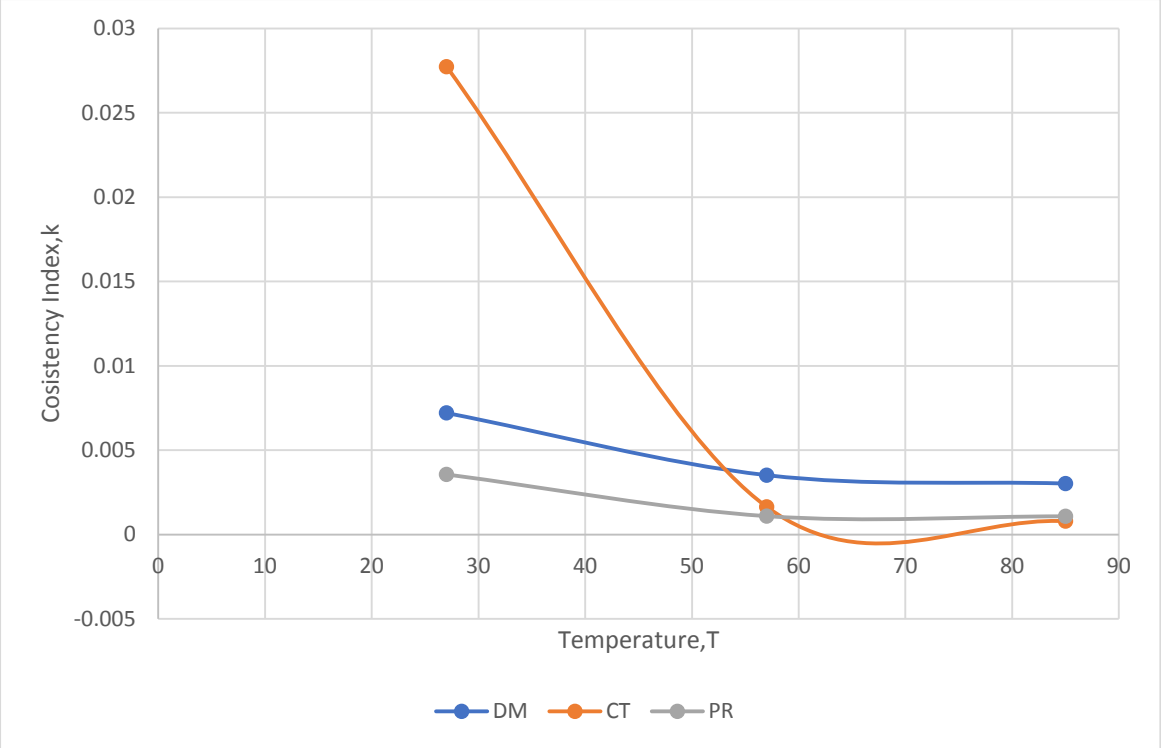

The consistency indicator, k of CT, indicates a drop in value. The PR and the DM consistency index, on the other hand, remains flat over the temperature range. This demonstrates PR and DM's efficacy at greater temperatures. The temperature denaturing problem that is associated with CT, may most likely not occur in DM and PR.

Drag Force and Settling Velocity
$g=9.81ms^{-1}$, d=0.002m, $\rho=19000kgm^{-3}$,

Table 4: Summary of results from the drag force and settling velocity experiment

	Reynold number, Re	Bingham number, Bi	Drag coefficient, CD	The drag force, F_D (N) x 10^{-5}	Settling velocity, v (mm/s)
DM	**84**	**243**	**5485.86**	**5.415**	**2.5**
CT	**3.05**	**264.8**	**40,679**	**4.205**	**0.8**
PR	**72**	**220**	**5365.86**	**4.415**	**2.4**

The proppant handling capability of the three polymers is shown in Table 4. Equations 8 through 13 were used to create the table. The best drag or buoyancy force is 4.415 x 10^{-5}N for PR. This means that the polymer sediment has the least potential to settle out of the solution. The settling or terminal velocity is best with CT, which has the slowest settling velocity of 0.8mm/s and hence will settle out of its solution in the shortest amount of time.

Conclusions

From this work, the following findings can be drawn:

i. The Hershel Bulkley fluid behaviors were seen in the carrier fluid made from the three polymers.

ii. The flow behavior index for the three polymers was calculated, and it was discovered that the flow behavior index increased as the temperature rose. At a concentration loading of 10g/l, the commercial CT had the highest values, followed by PR, and then DM.

iii. The flow consistency index, on the other hand, declines as temperature rises for all three polymers, with no clear trend within the polymer.

iv. At greater shear rates, CT has the highest rheology and is still the best polymer.

v. At higher temperatures, the PR demonstrated the highest rheology, suggesting that it could be the best substitute for CT.

vi. At higher temperatures, the PR had the highest rheology and could be the best substitute for CT.

vii The best drag force is PR, while the optimal settling velocity is CT.

viii. The DM is ineffective as a replacement for commercial CT.

COMPETING INTERESTS DISCLAIMER:

Authors have declared that no competing interests exist. The products used for this research are commonly and predominantly use products in our area of research and country. There is absolutely no conflict of interest between the authors and producers of the products because we do not intend to use these products as an avenue for any litigation but for the advancement of knowledge. Also, the research was not funded by the producing company rather it was funded by personal efforts of the authors.

Reference

Al-Muntasheri G (2014). *A critical review of hydraulic fracturing fluids over the last decade*. A paper was prepared for presentation at the SPE Western North American and Rocky Mountain joint regional meeting held in Denver Colorado, USA, 16-18 April 2014.SPE 169552.Pp 1-4.

Antosik, A, Glusek, M, Zurowski, R and Szafran, M (2017). Influence of carrier fluid on the electrokinetic and rheological properties of shear thickening fluids. Ceramics International.http//dx.doi.org/10.1016/j.ceramint.2017.06.092

Atapattu D, Chhabra R, and Uhlherr P (1995). Journal of Non-Newtonian Fluid Mechanics.59(1995)245.

Barati R (2014). A Review of Fracturing Fluid systems used for Hydraulic Fracturing of oil and gas wells. *Journal of Applied Polymer Science.* Pp1-11

Brannon D, Ault G (1991). *New, delayed borate-crosslinked fluid provide improved fracture conductivity in high-temperature applications*. A paper presented at the 66th Annual Technical Conference and Exhibition of the Society of Petroleum Engineers held in Dallas, TX, October 6-9, 1991.

Bo, C, Yun, X, Chunming, H, Yuebin, G, Guifu, D, Wei, J, Xuemei, Y and Zhihe,J (2018).A new High Temperature polymer fracturing fluid. IOP conference series: Earth and Environmental Science 186(2018)012028, doi:10.1088/1755-1315/186/4/012028

Cao X, Shi Y, Li W, Zeng P, Zheng Z, Feng Y and Yin H (2021). Comparative studies on Hydraulic Fracturing Fluids for high temperatures and high salt oil reservoirs Synthetic Polymer Vs Guar Gum. http://pubs.acs.org/journal/acsodf

Du, J, Xiang, K, Zhao, L, Lan, X, Liu, P, Liu, Y (2019). Synthesis and characterization of a novel, pH responsive, bola-based dynamic crosslinked fracturing fluid. Royal society of chemistry, Doi: 10.1039/c9ra02853f

Economides M and Nolte K (2000). *Reservoir Stimulation*. NY and Chichester.3rd ed., Wiley.

Geri M, Imqam A, and Flori R (2019). A Critical Review of Using High Viscosity Friction Reducers as Fracturing Fluids for Hydraulic Fracturing Application. A paper was prepared for presentation at the SPE Oklahoma City Oil and Gas Symposium held in Oklahoma City, Oklahoma, USA, 9-10 April 2019. SPE-195191-MS
http://www.bionicsscientific.com/sieve-shakers/test-sieves.html 23rd August 2021 12:57 PM

Iherijirika B, Dosunmu A and Eme C (2015). *Performance evaluation of guar gum as a carrier fluid for hydraulic fracturing*. A paper prepared for presentation at the Nigeria Annual International Conference and Exhibition held in Lagos, Nigeria.4-6 August 2015

Ma X, Wang H, Boyd W, Cheng M, Yao C and Lei G (2018).Thermal stability enhancement of guar-based hydraulic fracturing fluids by phosphate treatment. Journal of applied polymer science, Doi:10.1002/app.47119

Nwokocha L and Williams P (2009). Isolation and Rheological Characterization of *Mucuna flagellipes* Seed Gum. *Food Hydrocolloids*, 23(5), 1394-1397

Nwokocha L and Williams P (2012). Evaluating the potential of Nigerian Plants as a source of industrial hydrocolloids. In: Gums and Stabilizers for the food industry 16. G.O. Philips and P.A Williams (Editors). Royal Society of Chemistry, Cambridge, United Kingdom. Pp.31-34

Nwokocha L and Nwokocha K (2020). Chemical composition and rheological properties of *Detarium microcarpum* and *Irvingia gabonensis* seed flours. https://doi.org/10.1016/j.sciaf.2020.e00529 Published by Elsevier B.V. on behalf of African Institute of Mathematical Sciences / Next Einstein Initiative.

Robert M and Pin T (1993). Enzyme breaker for galactomannan-based fracturing fluid. USA Patent 5201370, 13 April 1993.

Recommended Practices for Measurement of the Viscous properties of Completion Fluids. API Recommended Practice 13M (R2018). Exploration and Production Department.

Uhegbu F, Onwuchekwa C,Iweala E and Kanu I(2009) . Effect of processing methods on nutritive and antinutritive properties of seeds of *Brachystegia eurycoma* and *Detarium microcarpum* from Nigeria,Pak.j.Nutr.8(4)(2009).316-320

Uzoma A and Odusanya O (2011). Mucuna sloanei,Detarium microcarpum and Brachystegia eurycoma seeds : A preliminary study of their starch-hydrocolloids system,Afr.J.Food Sci. 5(13)(2011) 733-740.

Worlow W and Holditch A (1989). *Rheological measurement of a crosslinked fracture fluid under conditions expected during fracture treatment*. A paper was prepared for presentation at the SPE Joint Rocky Mountain Regional Low Permeability Reservoirs Symposium and Exhibition held in Denver, Colorado. March 6-8,1989. SPE 18970 PP425-436

Zhao, L, Chen, Y, Du, J, Liu, P, Li, N, Luo, Z, Zhang, C (2019). Experimental study on a new type of self-propping fracturing technology. https://doi.org /10.1016/energy.2019 /j.energy .2019.06.137,PP.1-3.

Zhang, Y, Mao, J, Zhao, J, Xu, T, Du, A, Zhang, Z, Zhang, W and Ma, S (2019). Preparation of a novel fracturing fluid system with excellent elasticity and low friction. Polymers 2019,11,153

Appendix 1

Table 1 Rheology of *Detarium microcarpum* at 27°C, 57°C and 85°C

RPM	80°F	135°F	185°F

Θ600 (cP)	7	5	4
Θ300 (cP)	5	3	3
Θ200 (cP)	3	3	2
Θ100 (cP)	2	2	2
Θ6 (cP)	2	2	2
Θ3 (cP)	2	2	2
10 Secs (lb/100ft^2)	2	2	2
10 Mins (lb/100ft^2)	3	2	2
PV (cP)	2	2	1
YP (lb/100ft^2)	3	1	2
Density (ppg)	8.39	-	-

Table 2: Rheology of C. tetragonoloba at 27^{o}C, 57^{o}C and 85^{o}C

RPM	**27^{o}C**	**57^{o}C**	**85^{o}C**
Θ_{600} (cp)	71	64	52
Θ_{300} (cp)	51	35	27
Θ_{200} (cp)	42	28	16
Θ_{100} (cp)	30	16	11
Θ_{6} (cp)	6	4	3
Θ_{3} (cp)	5	3	2
10 secs (lb/100ft^2)	5	3	2
10 mins (lb/100ft^2)	7	4	3
PV (cp)	20	29	25
YP(lb/100ft$^{2)}$	31	6	2
Density (ppg)	8.3		

Table 3 : Rheology of PAC R at 27°C, 57°C and 85°C

RPM	27°C	57°C	85°C
Θ600 (cP)	44	42	38
Θ300 (cP)	27	23	21
Θ200 (cP)	20	19	17
Θ100 (cP)	12	10	9
Θ6 (cP)	3	3	2
Θ3 (cP)	3	3	2
10 Secs (lb/100ft^2)	4	4	3
10 Mins (lb/100ft^2)	5	4	3
PV (cP)	17	19	17
YP (lb/100ft^2)	10	4	4
Density (ppg)	8.1		

Appendix 2

Table 4 ASTM Conversion table for sieve sizes

Sieve Mesh Chart			
APERTURE SIZE			
B.S.S(410/1969)	**A.S.T.M. (11-70)**	**I.S. (469/1972)**	**MICRONS**
4	5	4.00mm	4000
5	6	3.35mm	3353
6	7	2.80mm	2812
7	8	2.36mm	2411
8	10	2.00mm	2057
10	12	1.70mm	4000
12	14	1.40mm	1405
14	16	1.18mm	1204
16	18	1.00mm	1204
18	20	0.850mm	850
22	25	0.710mm	710
25	30	0.600mm	600
30	35	0.500mm	500
36	40	0.425mm	420
44	45	0.355mm	355
52	50	0..300mm	300
60	60	0.250mm	250
72	70	0.212mm	210
85	80	0.180mm	180
100	100	0.150mm	150
120	120	0.125mm	120
150	140	0.106mm	105
170	170	0.090mm	90
200	200	0.075mm	75
240	230	0.063mm	63
300	270	0.053mm	53
350	325	0.045mm	45
400	400	0.037mm	37
500	500	0.025mm	25

Table 5: Particle Distribution of 100g of Sand Particles (proppant) with Specific gravity of 19gcm^{-3}

S/N	STANDARD SIEVE SIZE	PAN WEIGHT (g)	PAN WEIGHT + PARTICLES	PARTICLES (g)	PARTICLES (%)

			(g)		
1	**ASTM 10**	464.38	542.78	78.40	78.40
2	**ASTM 18**	451.97	459.17	7.20	7.20
3	**ASTM 40**	434.80	446.03	11.23	11.23
4	**ASTM 140**	423.74	426.81	3.07	3.07
5	**ASTM 200**	293.85	293.90	0.05	0.05
6	**PAN**	230.33	230.38	0.05	0.05
TOTAL				**100.00**	**100.00**